

**1 of 1**

TITLE: ELASTIC PROPERTIES OF AMORPHOUS THIN FILMS STUDIED BY  
RAYLEIGH WAVES

AUTHOR(S): R. B. Schwarz  
J. B. Rubin

SUBMITTED TO: Eighth International Conference on Rapidly Quenched  
and Metastable Materials, Sendai, Japan,  
August 22-27, 1993

**DISCLAIMER**

This report was prepared as an account of work sponsored by an agency of the United States Government. Neither the United States Government nor any agency thereof, nor any of their employees, makes any warranty, express or implied, or assumes any legal liability or responsibility for the accuracy, completeness, or usefulness of any information, apparatus, product, or process disclosed, or represents that its use would not infringe privately owned rights. Reference herein to any specific commercial product, process, or service by trade name, trademark, manufacturer, or otherwise does not necessarily constitute or imply its endorsement, recommendation, or favoring by the United States Government or any agency thereof. The views and opinions of authors expressed herein do not necessarily state or reflect those of the United States Government or any agency thereof.

By acceptance of this article, the publisher recognizes that the U.S. Government retains a nonexclusive, royalty-free license to publish or reproduce the published form of this contribution, or to allow others to do so, for U.S. Government purposes.

The Los Alamos National Laboratory requests that the publisher identify this article as work performed under the auspices of the U.S. Department of Energy

**Los Alamos** Los Alamos National Laboratory  
Los Alamos, New Mexico 87545

Keywords: Short-Range Order, Elastic Modulus, Rayleigh waves

## Elastic Properties of Amorphous Thin Films Studied by Rayleigh Waves

R.B. Schwarz and J.B. Rubin\*

Center for Materials Science, Mail Stop K765

Los Alamos National Laboratory,

Los Alamos, New Mexico 87545

### Abstract

Physical vapor deposition in ultra-high vacuum was used to co-deposit nickel and zirconium onto quartz single crystals and grow amorphous  $\text{Ni}_{1-x}\text{Zr}_x$  ( $0.1 < x < 0.87$ ) thin films. A high-resolution surface acoustic wave technique was developed for the in situ measurement of the film shear moduli. The modulus has narrow maxima at  $x = 0.17, 0.22, 0.43, 0.5, 0.63,$  and  $0.72$  reflecting short-range ordering and the formation of aggregates in the amorphous phase. It is proposed that the aggregates correspond to polytetrahedral atom arrangements which are limited in size by geometrical frustration.

### 1. Introduction

The experimental evidence for short-range order (SRO) in metallic liquids has been reviewed by Predel.[1] Based on observed variations in specific heat, activation energy for viscous flow, and other physical properties as a function of composition, Predel suggests that 'molecular aggregates' exist in the liquid state whose composition coincides with that of stable and metastable crystalline compounds. Based on the accumulated evidence, Predel [1] and Sommer [2] have proposed a theory for ordering in alloy melts of compound-forming systems. In their theory, an aggregate-forming alloy liquid can be characterized by a density of ordered aggregates dispersed within a 'sea' of randomly distributed (unassociated) atoms which form a truly amorphous liquid.

---

\* Present address: Microelectronics and Materials Technology Centre, Royal Melbourne Institute of Technology, Melbourne, 3001, Australia.

At any given temperature, the relative volume fractions of the aggregates and unassociated atoms are governed by the overall liquid composition and a law of mass action equilibrium, with the maximum volume fraction of aggregates occurring when the average liquid composition equals the stoichiometry of the aggregate.

The empirical data summarized by Predel [1] are for low-melting-temperature binary and ternary systems, since these melts are experimentally accessible by techniques such as calorimetry and x-ray diffraction. Analogous studies of high-melting-point systems present numerous experimental difficulties. To avoid some of these difficulties, researchers have used rapid solidification techniques to kinetically *freeze* the liquid structure into a glass. The SRO retained by the glass corresponds to that the liquid had at the *fictive* temperature  $T_f$  at which it became configurationally frozen.  $T_f$  is a function of the cooling rate.[3] Experiments conducted on splat-quenched and melt-spun amorphous alloys prepared at cooling rates between  $10^6$  and  $10^8$  K/s have confirmed the existence of SRO.[4]

In this paper we report the elastic properties of amorphous  $Ni_{1-x}Zr_x$  thin films. The films were prepared by the condensation of nickel and zirconium vapors in an ultra-high vacuum (UHV). The effective cooling rate for this technique is of the order of  $10^{12}$  K s<sup>-1</sup>, producing configurationally-frozen liquids over a continuous composition range ( $0.1 < x < 0.87$ ) which is much broader than that attainable by rapid quenching techniques.[5] Furthermore, these films should have a higher  $T_f$  and thus a lower degree of SRO than metallic glasses prepared by rapid quenching. Because these films are only 25 nm thick, exposing them to air and forming a surface oxide layer would have perturbed the measurements. To avoid this, the elastic measurement were done in situ (at pressures close to  $10^{-10}$  Torr) using a surface acoustic wave (SAW) method. For  $x < 0.1$  and  $x > 0.87$ , the films are nickel-rich and zirconium-rich crystalline solid solutions. The elastic properties of these films will be presented separately.

## 2. Experimental

The depositions were made onto "ST-cut" single-crystal  $\alpha$ -quartz substrates. A pair of interdigital transducers (Fig. 1) were deposited onto the surface of the substrata by photolithography. The SAW wavelength,  $\Lambda = 60$   $\mu$ m, is determined by twice the individual electrode width and

spacing. The Rayleigh wave velocity for ST-cut quartz is  $V_R = 3158 \text{ m s}^{-1}$  and therefore the center operating frequency of the devices is 52.63 MHz. The SAW devices contain fifty electrode pairs and can operate from approximately 51 to 53 MHz. The substrates are positioned in the UHV deposition chamber inside a ceramic holder, which has electrical feedthroughs for the input (send) and output (receive) signals.

The amorphous  $\text{Ni}_{1-x}\text{Zr}_x$  films were produced by simultaneous electron-beam evaporation from separate nickel and zirconium sources. The depositions were made upwards through a mask, which was held just below the surface of the substrate. The deposition rate of each material was independently controlled by quartz-crystal thickness monitors having a resolution of 0.01 nm. These monitors were carefully calibrated using Rutherford backscattering spectrometry. All of the alloy films had a thickness of 22.5 nm. The base pressure of the evaporation chamber was  $< 1 \times 10^{-9}$  Torr, and rose to  $5 \times 10^{-8}$  Torr during deposition. To obtain alloy films of different compositions, the evaporation rates of the sources were varied from 0.01 to 0.2  $\text{nm s}^{-1}$  for Ni, and from 0.01 to 1.0  $\text{nm s}^{-1}$  for Zr.

The elastic properties of the thin films were determined by measuring changes in  $V_R$  caused by the deposition of the films. Depending on the elastic properties of the film, adding a thin film to an ST-cut quartz substrate will either increase or decrease  $V_R$ . [6] Elemental nickel, elemental zirconium, and amorphous  $\text{Ni}_{1-x}\text{Zr}_x$  are all elastically softer than quartz and decrease  $V_R$ .

In general, the velocities of Rayleigh waves depend sensitively on substrate temperature and thus changes in temperature can severely degrade the accuracy and sensitivity of the measurements. The ST-cut orientation of the quartz substrata is designed to give  $dV_R/dT = 0$  near ambient temperature. Using a computer-controlled phase-lock loop the stability of the system is better than 1 part in  $10^6$ . [7] With this method, changes in  $V_R$  are related to changes in the carrier frequency by

$$\frac{\Delta V_R}{V_R} = \frac{L}{L_f} \frac{\Delta \omega}{\omega} \quad (1)$$

where  $L_f$  is the length of the film in the propagation direction, and  $L$  is the interdigital transducer spacing (see Fig. 1).

The elastic properties of (isotropic) amorphous thin films are characterized by only two elastic moduli. A first-order perturbation analysis [8] shows that for  $h \ll \Lambda/2\pi$ , where  $h$  is the film thickness and  $\Lambda$  is the Rayleigh wavelength. The change in frequency,  $\Delta\omega/\omega$ , is related to the elastic properties of an isotropic film by the expression:

$$\frac{\Delta V_R}{V_R} = \frac{V_R h}{4P_R} \left[ \left( \rho - \frac{\mu}{V_R^2} \right) \cdot |v_x|^2 + \rho |v_y|^2 + \left( \rho - \frac{4\mu}{V_R^2} \frac{\lambda + \mu}{\lambda + 2\mu} \right) \cdot |v_z|^2 \right], \quad (2)$$

where  $\rho$  is the film density, and the quantities  $v_x^2/4P_R$ ,  $v_y^2/4P_R$ , and  $v_z^2/4P_R$  are the normalized particle velocity components at the substrate surface.  $\lambda$  and  $\mu$  are the Lamé constants of the film, which are related by  $\lambda = 2\nu(\mu - 2\nu)^{-1}$ , where  $\nu$  is Poisson's ratio.

Equation (2) shows that  $V_R$  depends both on  $\lambda$  and  $\mu$ . However, using Eq. (2) it can be shown that

$$\frac{\partial \left( \frac{\Delta V_R}{V_R} \right)}{\partial \ln \mu} > 5 \frac{\partial \left( \frac{\Delta V_R}{V_R} \right)}{\partial \ln \lambda}, \quad (3)$$

so that  $V_R$  is much more sensitive to changes in  $\mu$  than in  $\lambda$ . This is due to the nature of the Rayleigh waves, where the particle displacements are elliptical with a large vertical eccentricity.

Using the relation between  $\lambda$ ,  $\mu$ , and  $\nu$ , we express  $\Delta V_R/V_R$  in Eq. (2) in terms of  $\mu$  and  $\nu$ . Based on previous work [9], we assume for amorphous NiZr alloys a Poisson's ratio value  $\nu = 0.35$ , independent of composition. Equation 2 is then used to evaluate the shear modulus  $\mu$  of the amorphous films from the measured values of  $\Delta V_R/V_R$ .

### 3. Results

Equation 2 predicts that the frequency changes caused by the deposited films should be linearly proportional to their thickness. Figure 2 shows decreases in frequency produced by varying thicknesses of elemental Ni, elemental Zr, and coevaporated amorphous  $\text{Ni}_{0.68}\text{Zr}_{0.32}$  films, along with the best fitted lines drawn through each data sets. The observed linear dependence of the

frequency change on film thickness enabled us to use Eq. (2) with confidence. Notice further that the shear modulus of the amorphous films is significantly lower than the average of the moduli of polycrystalline nickel and zirconium.

Figure 3 shows the measured values of  $\mu$  for amorphous films of  $\text{Ni}_{1-x}\text{Zr}_x$  of thickness  $h = 22.5$  nm. The arrows on the top of the figure defines the composition regime  $0.1 < x < 0.87$  where co-deposition produces a single-phase amorphous alloy. This range was deduced from resistivity and electron microscopy measurements reported separately.[10] Outside this regime, the alloy films are crystalline nickel-rich and zirconium-rich solid solutions, respectively. Also shown in this figure are vertical dotted lines denoting the compositions at which the Ni-Zr system forms, in equilibrium, crystalline intermetallics. On cooling the melt, the intermetallics  $\text{Ni}_7\text{Zr}_2$ ,  $\text{NiZr}$ , and  $\text{NiZr}_2$  freeze congruently, whereas  $\text{Ni}_5\text{Zr}$  and  $\text{Ni}_{10}\text{Zr}_7$  form through peritectic reactions. The open symbol is the shear modulus of polycrystalline  $\text{NiZr}_2$  deduced from the single crystal data.[11]

Each data point in Fig. 3 represents an independent shear modulus measurement. Successively measurements were taken at widely different compositions to avoid systematic errors and to verify that the thickness limit for the applicability of the linear perturbation theory (Eq. 2) had not been exceeded. We traced a continuous curve through the 72 data points to facilitate the discussion of the data.

#### 4. Discussion

Rayleigh waves have been used previously to study the elastic properties of thin films [12], but the present technique offers a substantial improvement in resolution, about 1 part in  $10^6$ , as compared to about 1 part in  $10^4$  for previous measurements. The added sensitivity enabled us to work in a lower frequency range ( $\approx 52$  MHz) where the Rayleigh wavelength ( $\Lambda \approx 60$   $\mu\text{m}$ ) greatly exceeded the thickness of the films being studied ( $h = 22.5$  nm). Working at lower frequencies enabled us to (1) deduce the absolute value of  $\mu(x)$  of the films without the need for approximate correction factors to account for the elastic contribution from the substrate and (2) to use of a perturbation theory analysis and to deposit films in succession onto the same substrate, yet to analyze them independently.



There is extensive experimental evidence for chemical and/or topological SRO in amorphous alloys of an early- and a late-transition metal [13,14,15,16] which cannot be discussed in this short paper. In these studies, the effects of SRO appear as *broad* changes in the quantity being measured which contrasts with the large number of rather *sharp* maxima of the present shear moduli measurements. The reason why sharp maxima had not been seen previously may be due to (1) the lower  $T_f$  in the splat quenched alloys and/or (2) the relatively small number of data taken at a reduced number of compositions.

Because the number of peaks in  $\mu(x)$  is larger than the number of singularities reported in any previous study, the question arises: do the number and sharpness of the singularities depend on the sample preparation method? The NiZr thin films were formed by the condensation of metal vapors. Although molecular dynamic modeling suggests that during vapor condensation the atoms go through a liquid-like state, the two-dimensional freezing may affect the type of SRO that is frozen into the glassy phase. However, samples prepared by rapid quenching techniques go through a similar two-dimensional freezing. Previous work suggests that sharper singularities in properties are observed in alloys prepared at the fastest rates of quenching. Kroeger et al. [17] suggest that the sharp peak in the electronic density of states they observed in amorphous  $Ni_{1-x}Zr_x$  for  $0.63 < x < 0.64$  in samples prepared by splat quenching at cooling rates of about  $10^9 \text{ K s}^{-1}$  is absent in the data of Altounian et al. [18] because the latter samples were prepared by melt spinning which is associated with a somewhat slower cooling rate of about  $10^7 \text{ K s}^{-1}$ .

The presence of many sharp maxima in  $\mu(x)$  suggests that liquid NiZr can form a variety of aggregates. That the present peaks in  $\mu(x)$  are so sharp suggests that during vapor condensation the melt cannot tolerate large fluctuations in composition and thus the stoichiometry of the aggregates must be close to the average liquid composition. A combination of techniques such as small-angle scattering, EXAFS, and Mossbauer spectroscopy may be needed to fully characterize the structure of the aggregates. However, the available data suggests the structure of the simplest aggregates, as we discuss next.

The most stable configuration of four identical atoms interacting via pairwise central potentials is a tetrahedral one in which each sphere is in contact with the other three. The local atomic structure of liquids is formed primarily by aggregates of these tetrahedra.[19] The simplest

such configuration is one of five atoms arranged in two tetrahedra that share a face. Saw and Schwarz [20] used a dense random-packed model to calculate the radial distribution functions and their Fourier transforms, the partial interference functions, in amorphous  $\text{Ni}_{0.35}\text{Zr}_{0.65}$ . The effect of short range ordering was investigated by introducing random permutations of nearest-neighbor nickel-zirconium atom pairs in response to a lowering of the alloy's enthalpy. They observed the development of a pre-peak in the Ni-Ni partial interference function at  $Q \approx 19 \text{ nm}^{-1}$  which grew in intensity with increasing the number of atomic permutations and reproduced the experimental pre-peak measured by Fukunaga and co-workers.[15,16] A statistical analysis of the dense random packed model showed that the atom permutations enable the formation of double tetrahedra composed of three Zr atoms capped by two Ni atoms, thus having the stoichiometry  $\text{Ni}_2\text{Zr}_3$ . The  $\mu(x)$  data in Fig. 2 has a sharp maximum at the composition  $x = 0.63$  which suggests that such an arrangements may exist in liquid NiZr alloys.

The next simplest polytetrahedral arrangement is that of five tetrahedra joining at a common edge to form a pentagonal bipyramid of seven atoms. However, because the dihedral angle between two tetrahedral faces,  $\alpha = \cos^{-1}(1/3) = 70.53^\circ$ , is not an integer fraction of  $2\pi$ , the pentagonal bipyramid cannot form unless some of the atomic bonds stretch and others contract by a few percent. Although taking care of this geometrical *frustration* requires added energy, the polytetrahedral order is preferred in liquids over that involving the half octahedra found in compact crystalline structures. Because the frustration increases as more atoms are attached to the polytetrahedral cluster, building large polyhedral *crystals* of identical atoms becomes energetically unfavorable.

In liquid alloys of elements having different atomic sizes, some of the limitations of frustration can be relaxed. In liquid NiZr, frustration for the pentagonal bipyramid should be reduced if the larger Zr atoms form the 5-atom ring with the smaller Ni atoms located at the two apices. Thus, we should expect that pentagonal bipyramids would form at the composition  $\text{Ni}_2\text{Zr}_7$  (e.g.,  $x = 0.71$ ). The  $\mu(x)$  data in Fig. 3 has a sharp maxima at  $x = 0.73$ , suggesting that pentagonal bipyramids may exist in liquid  $\text{Ni}_{0.27}\text{Zr}_{0.73}$ .

Frustration and symmetry suggests that the aggregates that form in binary liquids and amorphous alloys should have stoichiometric compositions corresponding to simple rational numbers. Sommer and Predel suggest that the volume fraction of aggregates should be largest when the liquid

composition equals the composition of one of the intermetallic compounds that forms in equilibrium. However, because the aggregates are not constrained to long range order, there is no requirement for the atomic arrangement of the aggregates to coincide with that found in any of the equilibrium crystalline intermetallic compounds in the NiZr system. In fact,  $\mu(x)$  in Fig. 3 has no peak at the compositions  $x = 0.67$ , corresponding to the crystalline congruent-melting intermetallic NiZr<sub>2</sub>. Some of the compositions where  $\mu(x)$  has maxima ( $x = 0.17, 0.22, 0.43, \text{ and } 0.5$ ) does coincide with the composition of high melting temperature crystalline intermetallics. If at these compositions the structure of the liquid aggregate is a sub-unit of the crystal structure, as proposed by Sommer and Predel, crystallization should be particularly *easy*, making it difficult to undercool these melts. However,  $\mu(x)$  has also maxima at the compositions  $x = 0.63$  and  $0.73$  which are close to the compositions of deep eutectics. Crystallization at these compositions should be *difficult* because it may require the dissolution of the aggregates, solute partitioning, and the formation of atomic arrangements not favored in the liquid (e.g., octahedral groups in NiZr and hcp-Zr). Thus, Ni<sub>1-x</sub>Zr<sub>x</sub> melt should be easy to undercool at the composition of the two Zr-rich eutectics, as observed experimentally.

In summary, the presence of SRO aggregates in the melt may help crystallization (if the aggregates are sub-units of the crystal) or hinder it (if crystallization requires the dissolution of the aggregates and solute partitioning). Recently, researchers at the Tohoku University developed various multicomponent metallic alloys in which  $\Delta T = T_x - T_g$  is as large as 100 K [21]. The alloys with the largest  $\Delta T$  can be solidified into glasses at relatively low quenching rates, enabling the synthesis of bulk amorphous alloys. The present results suggest that the narrow composition ranges at which easy glass formation is possible may correspond to the particular compositions at which the liquid develops especially strong chemical and topological SRO. Glass formation would be easy at this composition because for the liquid to crystallize it must first reconstruct its short range order to form the crystalline structure. The stronger the liquid SRO, the harder the reconstruction becomes, and this should facilitate the undercooling of the melt.

### **Acknowledgments**

This research was supported by the US Department of Energy, Office of Basic Energy Sciences, and through LANL Directed Research and Development funds.

---

## References

1. B. Predel, in Y. A. Chang and J. F. Smith (eds.), *Calculation of Phase diagrams and Thermochemistry of Alloy Phases*, AIME, Warrendale, PA, 1979, p. 72.
2. F. Sommer, *Z. Metallkd.*, 73 (1982) 72 and 77.
3. E. Balanzat and J. Hilairet, *J. Phys. F: Metal Phys.*, 12 (1982) 2907.
4. F. E. Luborsky, *Amorphous Metallic Alloys*, Butterworths, London, 1983.
5. C.-J. Lin and F. Spaepen, *Acta Metall.*, 34 (1986) 1367.
6. G. W. Farnell and E. L. Adler in W. P. Mason and R. N. Thurston (eds.), *Physical Acoustics*, Academic Press, New York, 1972, Vol. 9.
7. J. B. Rubin, Ph. D. Thesis, New Mexico Institute of Mining and Technology, 1992.
8. B. A. Auld, *Acoustic Fields and Waves in Solids*, Wiley, New York, 1973. Vol 2, p. 271.
9. H. -U. Künzi, in H. Beck and H. -J. Güntherodt, (eds.), *Glassy Metals II*, Springer-Verlag, Berlin, 1983, p. 169.
10. J. B. Rubin and R. B. Schwarz, *Mat. Res. Soc. Symp. Proc.*, 230 (1991) 21.
11. F. R. Eshelman and J. F. Smith, *J. Appl. Phys.*, 46 (1975) 5080.
12. M. Grimsditch in *Light Scattering in Solids V*, eds. M. Cardona and G. Guntherodt, Springer-Verlag, Berlin, 1989, p. 285.
13. H. S. Chen and J. T. Krause, *Scripta Metall.*, 11 (1977) 761.
14. R. Schulz, V. Matijasevic, and W. L. Johnson, *Phys. Rev.*, B30 (1984) 6856.
15. T. Fukunaga, N. Watanabe, and K. Suzuki, *J. Non-Cryst. Solids*, 61&62 (1984) 343.
16. T. Fukunaga, N. Hayashi, K. Kai, N. Watanabe, and K. Suzuki, *Physica B*, 120 (1983) 352.
17. D. M. Kroeger, C. C. Koch, J. O. Scarbrough, and C. G. McKamey, *Phys. Rev. B.*, 29 (1984) 1199.
18. Z. Altounian and J. O. Strom-Olsen, *Phys. Rev.*, B27 (1983) 4149.
19. D. R. Nelson and F. Spaepen in H. Ehrenreich and D. Turnbull (eds.), *Solid State Physics*, Academic Press, Boston, Vol. 42., p. 1.
20. C.K. Saw and R.B. Schwarz, *J. Less Comm. Metals*, 140 (1988) 385.
21. T. Zhang, A. Inoue, and T. Masumoto, *Materails Trans. Jap. Inst. Metals*, 32 (1991) 1005.

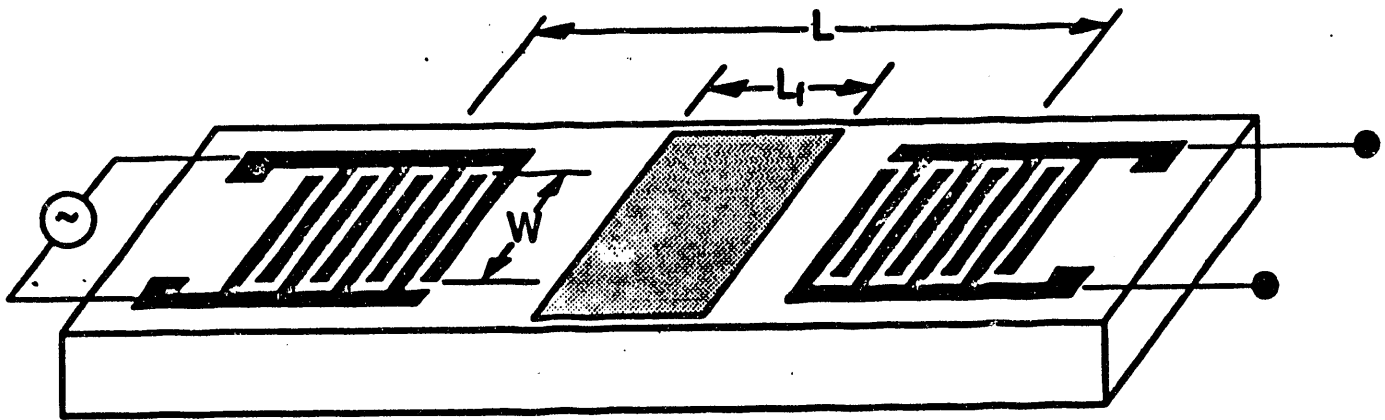


Fig. 1. (a) Schematic diagram of the piezoelectric substrate showing the configuration of the SAW electrodes.

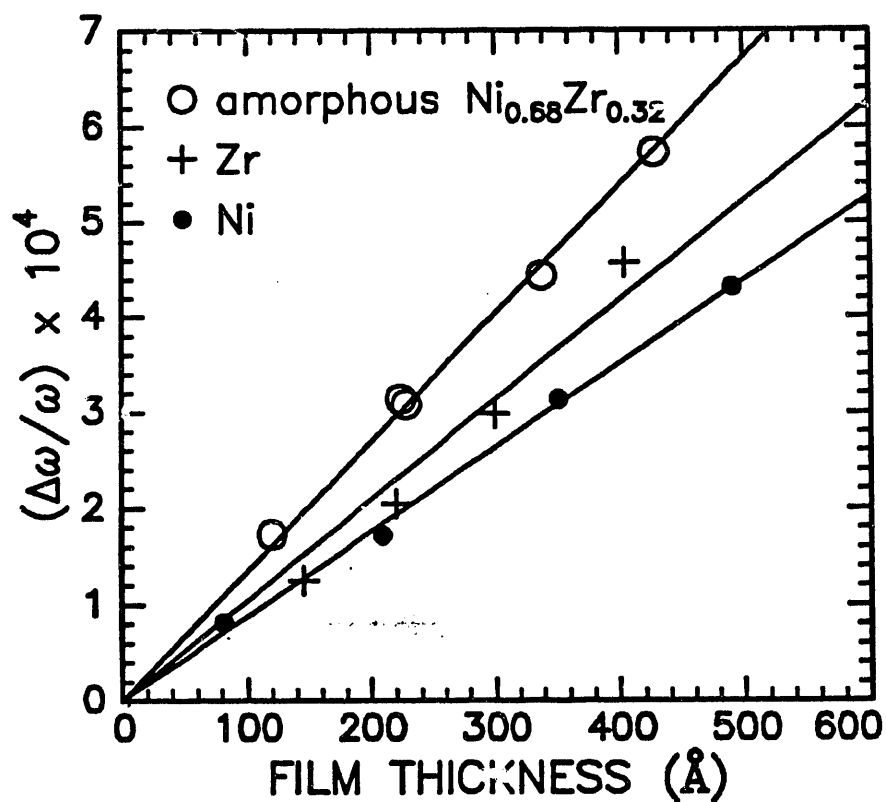
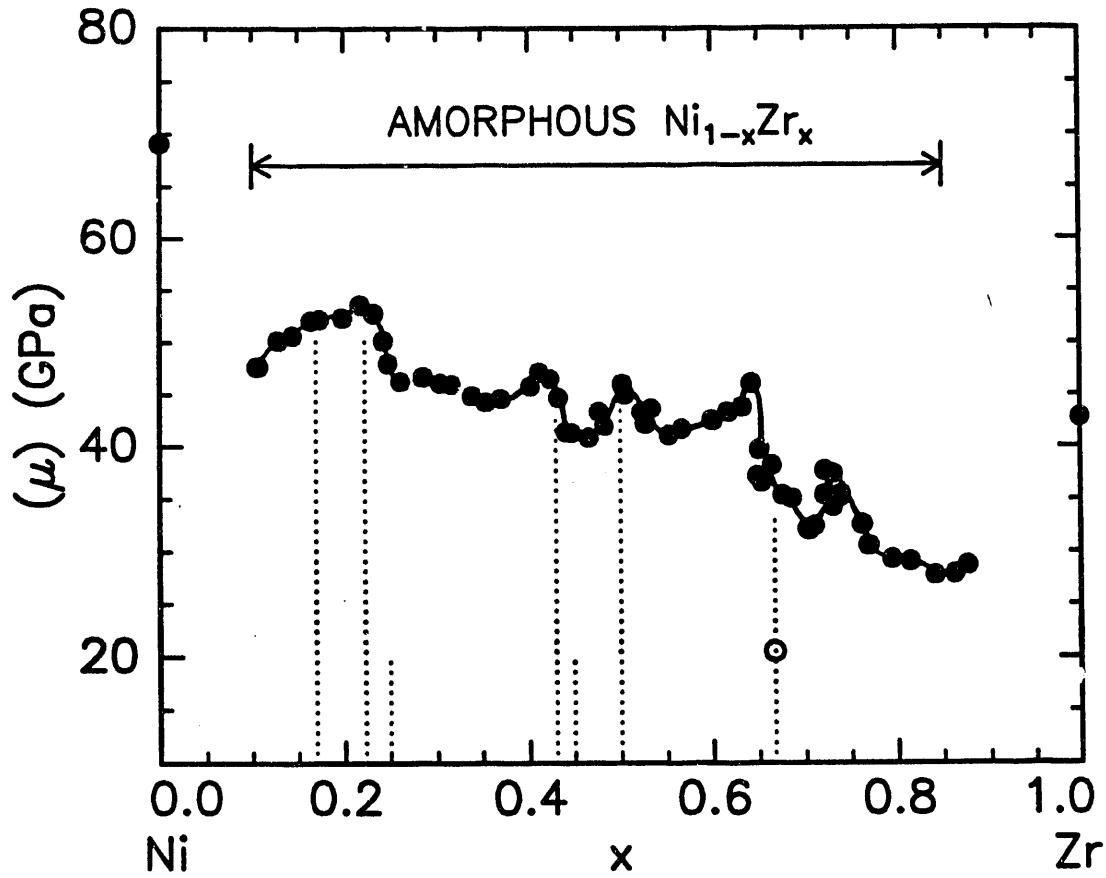


Figure 2. Decrease in the loop frequency  $\omega$  as a function of thickness for thin films of nickel, zirconium, and amorphous  $\text{Ni}_{0.68}\text{Zr}_{0.32}$ .



C:\genplot\macros\93nizram\shear.mac

Fig. 3. Shear moduli of amorphous  $\text{Ni}_{1-x}\text{Zr}_x$  alloy films. The dotted lines indicate the compositions at which Ni-Zr forms stable compounds. The open symbol is the shear modulus of polycrystalline  $\text{NiZr}_2$ .

**DATE  
FILMED**

*10 / 13 / 93*

**END**



